Istraživanja i projektovanja za privredu
ISSN 1451-4117
DOI:10.5937/jaes0-51432
www.engineeringscience.rs

iipp publishing

Journal of Applied Engineering Science
Vol. 22, No. 3, 2024
Original Scientific Paper
Paper number: 22(2024)3, 1231, 665-680

LONGITUDINAL VIBRATION ANALYSIS OF STRAIN GRADIENT ELASTIC BAR WITH VARIOUS BOUNDARY CONDITIONS

Vlasios Dimosthenis

Aristotle University of Thessaloniki, Faculty of Engineering, School of Civil Engineering, Hellas
** vlasdimo@civil.auth.gr*

In this paper, strain gradient elasticity (GradEla) is employed to investigate bar's longitudinal free vibration (LFV) behavior with several boundary conditions (BCs). The governing differential equation of motion for the bar is derived using Hamilton's principle. Various combinations of clamped, free, attached mass and/or spring BCs are used to solve it analytically. Notably, many of these solutions are the first in the literature for the gradient elastic bars. The effect of the internal length parameter, the modes, the attachments, the BCs, and the length of the bar is identified and assessed. It is concluded that the GradEla bar shows size-dependent and stiffer mechanical behavior compared with the classical one. Also, the presence of mass mainly decreases the longitudinal frequencies (LF) of bars, while the presence of the spring increases them. In addition, GradEla is applied to model a literature experiment demonstrating its applicability in real problems. Presenting these novel solutions and showcasing their effectiveness through experimental validation contributes to the advancement of understanding the use of GradEla theory in a wide range of longitudinal vibration (LV) problems of structural mechanics.

Keywords: longitudinal free vibration, bar, strain gradient elasticity, GradEla, boundary conditions

1 INTRODUCTION

The classical theory of elasticity is used in many engineering problems and applications. Over the years, the scale of the problems ranged from meters to nano-scale dimensions. In this nano-scale region, the mechanical behavior of materials is different from their behavior at macro-scales because the microstructural effects are significant. In addition, in the macro-scale region, there are cases where the macroscopic behavior is significantly affected by the microstructure of the material [1-2]. However, classical theory neglects the effect of microstructure and cannot predict its mechanical response correctly.

To deal with that problem, higher-order theories appeared. Like couple stress theories [3-5], strain gradient theories [6-8], nonlocal theories [9-11], and more recently modifications of them [12-13]. The insert of internal length scale parameters in the constitutive equations of classical theories can describe the materials' microstructure and size effects.

Aifantis and coworkers suggested a simple strain gradient model with only one additional constant in elasticity [14-16], widely known as GradEla. The linearized version of the stress-strain relation amounts to adding the Laplacian of the classical stress/strain expression into the standard form of Hooke's law and contains only one internal length-scale parameter, making the approach more convenient to be employed from physical and mathematical points of view.

Many researchers have used higher-order theories for solving bar problems. Following the GradEla theory, static and dynamic analysis of a bar has been studied by Altan et al. [17], Tsepoura et al. [18], and Parisis et al. [19]. Following the nonlocal theory of Eringen, the mechanical response of bars has been studied by Pisano and Fuschi [20], Aydogdu [21], Benvenuti and Simone [22], and Zhu and Li [23]. Numanuglu et al. [24] studied the LFVs of bars with several BCs according to Eringen's theory, in which the governing equations have the same order as the classical ones, and thus to find the solutions it follows the way of the classical theory. Kahrobaiyan et al. [25] and Akgoz and Civalek [26] studied the static and free vibration behavior of bars according to the modified gradient elasticity theory of Lam et al. [13]. However, to the authors' knowledge, no one studied the LFV behavior of the bar with various BCs, like attached mass and/or spring, using the GradEla theory, in which governing equations are of a higher-order, than the classical ones, making the use of higher-order BCs essential.

This paper investigates the LFV behavior of bars with various BCs based on the GradEla theory. The governing equation of motion is derived via Hamilton's principle. Several cases are solved with different combinations of BCs, like clamped, free, attached mass and/or spring, and the effects of internal length parameter, modes, attachments, BCs, and length on the frequencies of the bar are investigated and compared with the classical bar model. The GradEla theory is also used to model an experiment found in the literature, showcasing its applicability to real engineering problems.

The paper is organised as follows: In Section 2, the GradEla is introduced along with the equation of motion of the GradEla bar model, and it is studied its LFV behavior. In Section 3, a couple of case studies with different BCs are solved and discussed. Finally, conclusions are made in Section 4.

2 MATERIALS AND METHODS

2.1 GradEla theory

One of the most popular gradient elasticity theories is due to Aifantis and coworkers in the early 1990s, widely known as GradEla. Motivated by earlier work in plasticity [27-28] and nonlinear elasticity [14], Aifantis and coworkers suggested extending the linear elastic constitutive relations with the Laplacian of the strain as below [15-16,29]:

$$\sigma_{ij} = C_{ijkl}\left(\varepsilon_{kl} - \ell^2 \varepsilon_{kl,mm}\right) \tag{1}$$

where ℓ is again a length scale parameter of the material.

The strain energy density function, U, for isotropic, linearly elastic material reads:

$$U = \frac{1}{2}\lambda\varepsilon_{ii}\varepsilon_{jj} + \mu\varepsilon_{ij}\varepsilon_{ij} + \ell^2\left(\frac{1}{2}\lambda\varepsilon_{ii,k}\varepsilon_{jj,k} + \mu\varepsilon_{ij,k}\varepsilon_{ij,k}\right) \tag{2}$$

where λ and μ are the usual Lamé constants, $\varepsilon_{ij} = \frac{1}{2}\left(u_{i,j} + u_{j,i}\right)$ are the components of the infinitesimal strain, and ℓ is a strain gradient coefficient with dimensions of length.

For the bar model, the strain energy density function, U is given by:

$$U = \frac{1}{2}\int_0^L (\sigma\varepsilon + \sigma_x\varepsilon_x)Adx \tag{3a}$$

where the components of the stress tensors σ and σ_x, and the strain tensors ε and ε_x, are obtained as:

$$\sigma = E\frac{du(x,t)}{dx} \tag{3b}$$

$$\sigma_x = \ell^2 E\frac{d^2u(x,t)}{dx^2} \tag{3c}$$

$$\varepsilon = \frac{du(x,t)}{dx} \tag{3d}$$

$$\varepsilon_x = \frac{d^2u(x,t)}{dx^2} \tag{3e}$$

where E denotes elastic modulus, A the cross-section area, and ℓ the internal length parameter.

2.2 Governing equation and boundary conditions

For a bar with length L and cross-section A, the strain energy U, the kinetic energy T, and the variation of the work done by the external loads δW, are expressed as:

$$U = \frac{1}{2}\int_0^L \{EA\left(\frac{du(x,t)}{dx}\right)^2 + \ell^2 EA\left(\frac{d^2u(x,t)}{dx^2}\right)^2\}dx \tag{4}$$

$$T = \frac{1}{2}\int_0^L \rho A(\frac{du(x,t)}{dt})^2 dx \tag{5}$$

$$\delta W = \int_0^L q(x,t)\delta u dx + [P\delta u]_0^L + [R\delta\frac{du}{dx}]_0^L \tag{6}$$

where t denotes the time, ρ represents the density of the bar, q indicates the distributed axial load, and P and R refer to the conventional and higher-order axial resultants, respectively, acting on the end sections.

The governing equation and the BCs can be determined with the aid of Hamilton's principle:

$$\int_{t_1}^{t_2}\delta(U-T)dt - \int_{t_1}^{t_2}\delta W dt = 0 \tag{7}$$

According to the calculus of variation, the first integral of Eq. 7 can be written as:

$$\int_{t_1}^{t_2}\delta(U-T)dt = \int_{t_1}^{t_2}\int_0^L \delta F(u_x, u_{xx}, \dot{u})dx\,dt = \int_{t_1}^{t_2}\{\int_0^L [\frac{\partial^2}{\partial x^2}\left(\frac{\partial F}{\partial u_{xx}}\right) - \frac{\partial}{\partial x}\left(\frac{\partial F}{\partial u_x}\right) - \frac{\partial}{\partial t}\left(\frac{\partial F}{\partial \dot{u}}\right)]\delta u dx\}\,dt$$
$$+ \int_{t_1}^{t_2}\left[\left[\frac{\partial F}{\partial u_x} - \frac{\partial}{\partial x}\left(\frac{\partial F}{\partial u_{xx}}\right)\right]\delta u + \frac{\partial F}{\partial u_{xx}}\delta u'\right]_0^L dt + \int_0^L \left[\frac{\partial F}{\partial \dot{u}}\delta u\right]_{t_1}^{t_2} dx \tag{8}$$

The Lagrangian function for the present case is:

$$F = \frac{EA}{2}(u_x)^2 + \ell^2\frac{EA}{2}(u_{xx})^2 - \frac{\rho A}{2}(\dot{u})^2 \tag{9}$$

where $u_x = \frac{du}{dx}$, $u_{xx} = \frac{d^2u}{dx^2}$, and $\dot{u} = \frac{du}{dt}$.

Thus, Eq. 8 becomes:

$$\int_{t_1}^{t_2}\delta(U-T)dt = \int_{t_1}^{t_2}\{\int_0^L[\ell^2 EAu_{xxxx} - EAu_{xx} + \rho A\ddot{u}]\delta u dx\}dt + \int_{t_1}^{t_2}[(EAu_x - \ell^2 EAu_{xxx})\delta u + \ell^2 EAu_{xx}\delta u']_0^L dt + \int_0^L[\rho A\dot{u}\delta u]_{t_1}^{t_2}dx\} \tag{10}$$

The second integral of Eq. 7 can be written as:

$$\int_{t_1}^{t_2}\delta W dt = \int_{t_1}^{t_2}\int_0^L q(x,t)\delta u dx dt + \int_{t_1}^{t_2}\{[P\delta u]_0^L + [Q\delta u']_0^L\}dt \tag{11}$$

Because of Eqs. 10-11, Eq. 7 takes the form:

$$\int_{t_1}^{t_2}\{\int_0^L[\ell^2 EAu_{xxxx} - EAu_{xx} + \rho A\ddot{u}]\delta u dx\}dt + \int_{t_1}^{t_2}[(EAu_x - \ell^2 EAu_{xxx})\delta u + \ell^2 EAu_{xx}\delta u']_0^L dt + \int_0^L[\rho A\dot{u}\delta u]_{t_1}^{t_2}dx\} - \int_{t_1}^{t_2}\int_0^L q(x,t)\delta u dx dt + \int_{t_1}^{t_2}[P\delta u]_0^L + [Q\delta u']_0^L dt = 0 \tag{12}$$

Thus, the governing equation of a GradEla bar is derived as:

$$EA\frac{\partial^2 u}{\partial x^2} - \ell^2 EA\frac{\partial^4 u}{\partial x^4} + q = \rho A\frac{\partial^2 u}{\partial t^2} \tag{13a}$$

the initial conditions satisfy the equation

$$\frac{du(x,t_2)}{dt}\delta u(x,t_2) - \frac{du(x,t_1)}{dt}\delta u(x,t_1) = 0 \tag{13b}$$

and the BCs are

$$P = EA\frac{du}{dx} - \ell^2 EA\frac{\partial^3 u}{\partial x^3} \;\; or \;\; \delta u = 0 \quad at\; x = 0, L \tag{13c}$$

$$Q = \ell^2 EA\frac{\partial^2 u}{\partial x^2} \;\; or \;\; \delta u' = 0 \quad at\; x = 0, L \tag{13d}$$

It can be seen from Eq. 13a that the current GradEla bar model contains only one additional material parameter besides the two classical ones. The presence of ℓ in the new model enables the incorporation of the material size features and makes it possible to predict the size effect. Also, by setting $\ell = 0$, the proposed bar model will reduce to the classical one.

2.3 Longitudinal free vibration behavior

In this subsection, the LFV behavior of the GradEla bar is investigated. So, by considering $q = 0$, the Eq. 13a is taking the form:

$$EA\frac{\partial^2 u}{\partial x^2} - \ell^2 EA\frac{\partial^4 u}{\partial x^4} = \rho A\frac{\partial^2 u}{\partial t^2} \tag{14}$$

To solve the equation of motion Eq. 14, we assume a solution of the form:

$$u(x,t) = U(x)T(t) \tag{15}$$

and use the separation of variables method. Substituting Eq. 15 into 14 leads to:

$$\frac{E}{\rho U}\left(\frac{\partial^2 U}{\partial x^2} - l^2\frac{\partial^4 U}{\partial x^4}\right) = \frac{\frac{\partial^2 T}{\partial t^2}}{T} \tag{16}$$

The left-hand side of Eq. 16 depends only on x, and the right-hand side depends only on t. Assuming, their common value to be $-\omega^2$, Eq. 16 can be written as two separate equations:

$$\ell^2 \frac{\partial^4 U}{\partial x^4} - \frac{\partial^2 U}{\partial x^2} - \frac{\rho\omega^2}{E} U = 0 \tag{17a}$$

$$\frac{\partial^2 T}{\partial t^2} + \omega^2 T = 0 \tag{17b}$$

The general solution of Eq. 17a is:

$$U(x) = c_1 \cos s_1 x + c_2 \sin s_1 x + c_3 \cosh s_2 x + c_4 \sinh s_2 x \tag{18a}$$

where

$$s_1 = \sqrt{\frac{-1+\sqrt{4\ell^2\frac{\rho\omega^2}{E}+1}}{2\ell^2}} \quad \text{and} \quad s_2 = \sqrt{\frac{1+\sqrt{4\ell^2\frac{\rho\omega^2}{E}+1}}{2\ell^2}} = \sqrt{{s_1}^2 + \frac{1}{l^2}} \tag{18b}$$

and c_1, c_2, c_3, c_4 are constants to be determined from the BCs of the bar. Eq. 18a represents the normal mode.
The general solution of Eq. 17b is:

$$T(t) = c_5 \sin \omega t + c_6 \cos \omega t \tag{18c}$$

and c_5, c_6 are constants to be determined from the initial conditions of the bar. Eq. 18c indicates the harmonic motion.

3 RESULTS AND DISCUSSION

3.1 Case studies

In the present section, several BCs (displayed in Fig. 1), like clamped-free (C-F), clamped-clamped (C–C), clamped-attached mass (C-M), clamped-attached linear spring (C-S), clamped-attached mass and linear spring (C-MS), free-free (F-F), free-attached mass (F-M), free-attached linear spring (F-S), and free-attached mass and linear spring (F-MS) are studied.

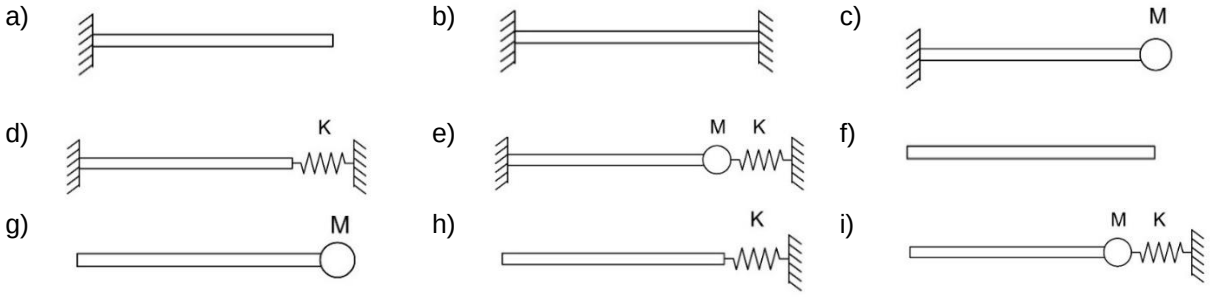

Fig. 1. Bar models with different BCs a) C-F, b) C-C, c) C-M, d) C-S, e) C-MS, f) F-F, g) F-M, h) F-S, i) F-MS

3.1.1 C-F boundary condition

The BCs for this case are:

$$u(0,t) = 0 \tag{19a}$$

$$\frac{\partial^2 u(0,t)}{\partial x^2} = 0 \tag{19b}$$

$$\frac{du(L,t)}{dx} - \ell^2 \frac{\partial^3 u(L,t)}{\partial x^3} = 0 \tag{19c}$$

$$\frac{du(L,t)}{dx} = 0 \tag{19d}$$

Applying the BCs of Eqs. 19a-19b to Eq. 18a leads to: $c_1 = c_3 = 0$.
So, Eq. 18a becomes:

$$U(x) = c_2 \sin s_1 x + c_4 \sinh s_2 x \tag{20}$$

Applying the BCs of Eqs. 19c-19d to Eq. 20 and 15 leads to:

$$\begin{bmatrix} s_1 \cos s_1 L + \ell^2 {s_1}^3 \cos s_1 L & s_2 \cosh s_2 L - \ell^2 {s_2}^3 \cosh s_2 L \\ s_1 \cos s_1 L & s_2 \cosh s_2 L \end{bmatrix} \begin{bmatrix} c_2 \\ c_4 \end{bmatrix} = \begin{bmatrix} 0 \\ 0 \end{bmatrix} \tag{21}$$

For a nontrivial solution, the determinant of the coefficient matrix of Eq. 21 must be equal to zero.
So, it is derived the characteristic equation from which the natural frequency can be obtained:

$$\cos s_1 L = 0 \tag{22a}$$

So, to satisfy the Eq. 22a s_1 should be:

$$s_1 = \frac{(2n-1)\pi}{2L} \quad \text{with } n = 1,2,\ldots \tag{22b}$$

Thus, by inserting Eq. 22b in Eq. 18b, the natural LFs of the C-F bar are:

$$\omega_n = \frac{(2n-1)\pi}{2L}\sqrt{\frac{E}{\rho}}\sqrt{1+\ell^2\left(\frac{(2n-1)\pi}{2L}\right)^2} = \omega_n^{cl}\sqrt{1+\ell^2\left(\frac{(2n-1)\pi}{2L}\right)^2} \tag{23a}$$

where $\omega_n^{cl} = \frac{(2n-1)\pi}{2L}\sqrt{\frac{E}{\rho}}$ denotes the natural LF of the classical bar model, and n the number of the vibration mode.
Thus, the normalized LFs ${\omega_n}^n$ of the C-F bar are:

$${\omega_n}^n = \frac{\omega_n}{\omega_n^{cl}} = \sqrt{1+\ell^2(\frac{(2n-1)\pi}{2L})^2} \tag{23b}$$

3.1.2 C-C boundary condition

The BCs for this case are:

$$u(0,t) = 0 \tag{24a}$$

$$\frac{\partial^2 u(0,t)}{\partial x^2} = 0 \tag{24b}$$

$$u(L,t) = 0 \tag{24c}$$

$$\frac{\partial^2 u(L,t)}{\partial x^2} = 0 \tag{24d}$$

Applying the BCs of Eqs. 24a-24b to Eq. 18a leads to: $c_1 = c_3 = 0$.
So, Eq. 18a becomes:

$$U(x) = c_2 \sin s_1 x + c_4 \sinh s_2 x \tag{20}$$

Applying the BCs of Eqs. 24c-24d to Eq. 20 and 15 leads to:

$$\begin{bmatrix} \sin s_1 L & \sinh s_2 L \\ -{s_1}^2 \sin s_1 L & {s_2}^2 \sinh s_2 L \end{bmatrix}\begin{bmatrix} c_2 \\ c_4 \end{bmatrix} = \begin{bmatrix} 0 \\ 0 \end{bmatrix} \tag{25}$$

For a nontrivial solution, the determinant of the coefficient matrix of Eq. 25 must be equal to zero.
So, it is derived the characteristic equation from which the natural frequency can be obtained:

$$\sin s_1 L = 0 \tag{26a}$$

So, to satisfy the Eq. 26a s_1 should be:

$$s_1 = \frac{n\pi}{L} \quad \text{with } n = 1,2,\ldots \tag{26b}$$

Thus, by inserting Eq. 26b in Eq. 18b, the natural LFs of the C-C bar are:

$$\omega_n = \frac{n\pi}{L}\sqrt{\frac{E}{\rho}}\sqrt{1+\ell^2\left(\frac{n\pi}{L}\right)^2} = \omega_n^{cl}\sqrt{1+\ell^2\left(\frac{n\pi}{L}\right)^2} \tag{27a}$$

where $\omega_n^{cl} = \frac{n\pi}{L}\sqrt{\frac{E}{\rho}}$ denotes the natural LF of the classical bar model, and n the number of the vibration mode.
Thus, the normalized LFs ${\omega_n}^n$ of the C-C bar are:

$${\omega_n}^n = \frac{\omega_n}{\omega_n^{cl}} = \sqrt{1+\ell^2(\frac{n\pi}{L})^2} \tag{27b}$$

3.1.3 C-M boundary condition

The BCs for this case are:

$$u(0,t) = 0 \tag{28a}$$

$$u''(0,t) = 0 \tag{28b}$$

$$EA\left(\frac{du(L,t)}{dx} - \ell^2 \frac{\partial^3 u(L,t)}{\partial x^3}\right) = -M\frac{\partial^2 u(L,t)}{\partial t^2} \tag{28c}$$

$$\frac{du(L,t)}{dx} = 0 \tag{28d}$$

Applying the BCs of Eqs. 28a-28b to Eq. 18a leads to: $c_1 = c_3 = 0$.

So, Eq. 18a becomes:

$$U(x) = c_2 \sin s_1 x + c_4 \sinh s_2 x \tag{20}$$

Applying the BCs of Eqs. 28c-28d to Eqs. 20 and 15 leads to:

$$\begin{bmatrix} C_{11} & C_{12} \\ C_{21} & C_{22} \end{bmatrix} \begin{bmatrix} c_2 \\ c_4 \end{bmatrix} = \begin{bmatrix} 0 \\ 0 \end{bmatrix} \tag{29}$$

where

$C_{11} = EAs_1 \cos s_1 L\,(1 + \ell^2 {s_1}^2) - \omega^2 M \sin s_1 L$

$C_{12} = EAs_2 \cosh s_2 L\,(1 - \ell^2 {s_2}^2) - \omega^2 M \sinh s_2 L$

$C_{21} = s_1 \cos s_1 L$

$C_{22} = s_2 \cosh s_2 L$

For a nontrivial solution, the determinant of the coefficient matrix of Eq. 29 must be equal to zero.

So, it is derived the characteristic equation from which the natural frequencies of the C-M bar can be obtained:

$$(EAs_1 \cos s_1 L\,(1 + \ell^2 {s_1}^2) - \omega^2 M \sin s_1 L)(s_2 \cosh s_2 L) - (EAs_2 \cosh s_2 L\,(1 - \ell^2 {s_2}^2) - \omega^2 M \sinh s_2 L)(s_1 \cos s_1 L) = 0 \tag{30}$$

Eq. 30 is complex, so we follow a different procedure to find the natural frequencies. For a sequence of values of ω we solve Eq. 30 and observe which values are the roots. Those values are the natural frequencies, where the first root is the first frequency ω_1, the second root is the second one ω_2, and so on.

3.1.4 C-S boundary condition

The BCs for this case are:

$$u(0,t) = 0 \tag{31a}$$

$$\frac{\partial^2 u(0,t)}{\partial x^2} = 0 \tag{31b}$$

$$EA\left(\frac{du(L,t)}{dx} - \ell^2 \frac{\partial^3 u(L,t)}{\partial x^3}\right) = -Ku(L,t) \tag{31c}$$

$$\frac{du(L,t)}{dx} = 0 \tag{31d}$$

Applying the BCs of Eqs. 31a-31b to Eq. 18a leads to: $c_1 = c_3 = 0$.

So, Eq. 18a becomes:

$$U(x) = c_2 \sin s_1 x + c_4 \sinh s_2 x \tag{20}$$

Applying the BCs of Eqs. 31c-31d to Eqs. 20 and 15 leads to:

$$\begin{bmatrix} C_{11} & C_{12} \\ C_{21} & C_{22} \end{bmatrix} \begin{bmatrix} c_2 \\ c_4 \end{bmatrix} = \begin{bmatrix} 0 \\ 0 \end{bmatrix} \tag{32}$$

where

$C_{11} = EAs_1 \cos s_1 L\,(1 + \ell^2 {s_1}^2) + K \sin s_1 L$

$C_{12} = EAs_2 \cosh s_2 L\,(1 - \ell^2 {s_2}^2) + K \sinh s_2 L$

$C_{21} = s_1 \cos s_1 L$

$C_{22} = s_2 \cosh s_2 L$

For a nontrivial solution, the determinant of the coefficient matrix of Eq. 32 must be equal to zero.
So, it is derived the characteristic equation from which the natural frequencies of the C-S bar can be obtained:

$$(EAs_1 \cos s_1 L\,(1+\ell^2 {s_1}^2)+K\sin s_1 L)(s_2\cosh s_2 L)-(EAs_2\cosh s_2 L\,(1-\ell^2 {s_2}^2)+K\sinh s_2 L)(s_1\cos s_1 L)=0 \quad (33)$$

Eq. 33 is complex, so we follow the same procedure stated before to find its roots which are the natural frequencies.

3.1.5 C-MS boundary condition

The BCs for this case are:

$$u(0,t)=0 \quad (34a)$$

$$\frac{\partial^2 u(0,t)}{\partial x^2}=0 \quad (34b)$$

$$EA\left(\frac{du(L,t)}{dx}-\ell^2\frac{\partial^3 u(L,t)}{\partial x^3}\right)=-Ku(L,t)-M\frac{\partial^2 u(L,t)}{\partial t^2} \quad (34c)$$

$$\frac{du(L,t)}{dx}=0 \quad (34d)$$

Applying the BCs of Eqs. 34a-34b to Eq. 18a leads to: $c_1=c_3=0$.
So, Eq. 18a becomes:

$$U(x)=c_2\sin s_1 x+c_4\sinh s_2 x \quad (20)$$

Applying the BCs of Eqs. 34c-34d to Eqs. 20 and 15 leads to:

$$\begin{bmatrix}C_{11} & C_{12}\\ C_{21} & C_{22}\end{bmatrix}\begin{bmatrix}c_2\\ c_4\end{bmatrix}=\begin{bmatrix}0\\ 0\end{bmatrix} \quad (35)$$

where

$C_{11}=EAs_1\cos s_1 L\,(1+\ell^2 {s_1}^2)-\sin s_1 L\,(\omega^2 M-K)$

$C_{12}=EAs_2\cosh s_2 L\,(1-\ell^2 {s_2}^2)-\sinh s_2 L\,(\omega^2 M-K)$

$C_{21}=s_1\cos s_1 L$

$C_{22}=s_2\cosh s_2 L$

For a nontrivial solution, the determinant of the coefficient matrix of Eq. 35 must be equal to zero.
So, it is derived the characteristic equation from which the natural frequencies of the C-MS bar can be obtained:

$$\begin{aligned}&\left(EAs_1\cos s_1 L\,(1+\ell^2 {s_1}^2)-\sin s_1 L\,(\omega^2 M-K)\right)(s_2\cosh s_2 L)\\&\quad-\left(EAs_2\cosh s_2 L\,(1-\ell^2 {s_2}^2)-\sinh s_2 L\,(\omega^2 M-K)\right)(s_1\cos s_1 L)=0\end{aligned} \quad (36)$$

Eq. 36 is complex, so we follow the same procedure stated before to find the natural frequencies.

3.1.6 F-F boundary condition

The BCs for this case are:

$$\frac{du(0,t)}{dx}-\ell^2\frac{\partial^3 u(0,t)}{\partial x^3}=0 \quad (37a)$$

$$\frac{du(0,t)}{dx}=0 \quad (37b)$$

$$\frac{du(L,t)}{dx}-\ell^2\frac{\partial^3 u(L,t)}{\partial x^3}=0 \quad (37c)$$

$$\frac{du(L,t)}{dx}=0 \quad (37d)$$

Applying the BCs of Eqs. 37a-37b to Eq. 18a leads to: $c_2=c_4=0$.
So, Eq. 18a becomes:

$$U(x)=c_1\cos s_1 x+c_3\cosh s_2 x \quad (38)$$

Applying the BCs of Eqs. 37c-37d to Eq. 38 and 15 leads to:

$$\begin{bmatrix}-s_1\sin s_1 L\,(1+\ell^2 {s_1}^2) & s_2\sinh s_2 L\,(1-\ell^2 {s_2}^2)\\ -s_1\sin s_1 L & s_2\sinh s_2 L\end{bmatrix}\begin{bmatrix}c_1\\ c_3\end{bmatrix}=\begin{bmatrix}0\\ 0\end{bmatrix} \quad (39)$$

For a nontrivial solution, the determinant of the coefficient matrix of Eq. 39 must be equal to zero.
So, it is derived the characteristic equation from which the natural frequency can be obtained:

$$\sin s_1 L = 0 \tag{40a}$$

So, to satisfy the Eq. 22a s_1 should be:

$$s_1 = \frac{n\pi}{L} \quad \text{with } n = 1,2,\dots \tag{40b}$$

Thus, by inserting Eq. 40b in Eq. 18b, the natural longitudinal frequencies of the F-F bar are:

$$\omega_n = \frac{n\pi}{L}\sqrt{\frac{E}{\rho}}\sqrt{1+\ell^2\left(\frac{n\pi}{L}\right)^2} = \omega_n^{cl}\sqrt{1+\ell^2\left(\frac{n\pi}{L}\right)^2} \tag{41a}$$

where $\omega_n^{cl} = \frac{n\pi}{L}\sqrt{\frac{E}{\rho}}$ denotes the natural LF of the classical bar model, and n the number of the vibration mode.

Thus, the normalized LF ${\omega_n}^n$ of the F-F bar are:

$${\omega_n}^n = \frac{\omega_n}{\omega_n^{cl}} = \sqrt{1+\ell^2(\frac{n\pi}{L})^2} \tag{41b}$$

3.1.7 F-M boundary condition

The BCs for this case are:

$$\frac{du(0,t)}{dx} - \ell^2\frac{\partial^3 u(0,t)}{\partial x^3} = 0 \tag{42a}$$

$$\frac{du(0,t)}{dx} = 0 \tag{42b}$$

$$EA(\frac{du(L,t)}{dx} - \ell^2\frac{\partial^3 u(L,t)}{\partial x^3}) = -M\frac{\partial^2 u(L,t)}{\partial t^2} \tag{42c}$$

$$\frac{du(L,t)}{dx} = 0 \tag{42d}$$

Applying the BCs of Eqs. 42a-42b to Eq. 18a leads to: $c_2 = c_4 = 0$.
So, Eq. 18a becomes:

$$U(x) = c_1\cos s_1 x + c_3\cosh s_2 x \tag{38}$$

Applying the BCs of Eqs. 42c-42d to Eq. 38 and 15 leads to:

$$\begin{bmatrix} C_{11} & C_{12} \\ C_{21} & C_{22} \end{bmatrix}\begin{bmatrix} c_1 \\ c_3 \end{bmatrix} = \begin{bmatrix} 0 \\ 0 \end{bmatrix} \tag{43}$$

where
$C_{11} = -EAs_1\sin s_1 L\,(1+\ell^2{s_1}^2) - M\omega^2\cos s_1 L$
$C_{12} = EAs_2\sinh s_2 L\,(1-\ell^2{s_2}^2) - M\omega^2\cosh s_2 L$
$C_{21} = -s_1\sin s_1 L$
$C_{22} = s_2\sinh s_2 L$
For a nontrivial solution, the determinant of the coefficient matrix of Eq. 43 must be equal to zero.
So, it is derived the characteristic equation from which the natural frequencies of the F-M bar can be obtained:

$$(-EAs_1\sin s_1 L\,(1+\ell^2{s_1}^2) - M\omega^2\cos s_1 L)(s_2\sinh s_2 L) + (EAs_2\sinh s_2 L\,(1-\ell^2{s_2}^2) - M\omega^2\cosh s_2 L)(s_1\sin s_1 L) = 0 \tag{44}$$

Eq. (44) is complex, so we follow the same procedure stated before to find the natural frequencies.

3.1.8 F-S boundary condition

The BCs for this case are:

$$\frac{du(0,t)}{dx} - \ell^2\frac{\partial^3 u(0,t)}{\partial x^3} = 0 \tag{45a}$$

$$\frac{du(0,t)}{dx} = 0 \tag{45b}$$

$$EA\left(\frac{du(L,t)}{dx} - \ell^2 \frac{\partial^3 u(L,t)}{\partial x^3}\right) = -Ku(L,t) \tag{45c}$$

$$\frac{du(L,t)}{dx} = 0 \tag{45d}$$

Applying the BCs of Eqs. 45a-45b to Eq. 18a leads to: $c_2 = c_4 = 0$.
So, Eq. 18a becomes:

$$U(x) = c_1 \cos s_1 x + c_3 \cosh s_2 x \tag{38}$$

Applying the BCs of Eqs. 45c-45d to Eq. 38 and 15 leads to:

$$\begin{bmatrix} C_{11} & C_{12} \\ C_{21} & C_{22} \end{bmatrix} \begin{bmatrix} c_1 \\ c_3 \end{bmatrix} = \begin{bmatrix} 0 \\ 0 \end{bmatrix} \tag{46}$$

where

$C_{11} = -EAs_1 \sin s_1 L\,(1 + \ell^2 {s_1}^2) + K \cos s_1 L$

$C_{12} = EAs_2 \sinh s_2 L\,(1 - \ell^2 {s_2}^2) + K \cosh s_2 L$

$C_{21} = -s_1 \sin s_1 L$

$C_{22} = s_2 \sinh s_2 L$

For a nontrivial solution, the determinant of the coefficient matrix of Eq. 46 must be equal to zero.
So, it is derived the characteristic equation from which the natural frequencies of the F-S bar can be obtained:

$$(-EAs_1 \sin s_1 L\,(1 + \ell^2 {s_1}^2) + K \cos s_1 L)(s_2 \sinh s_2 L) + (EAs_2 \sinh s_2 L\,(1 - \ell^2 {s_2}^2) + K \cosh s_2 L)(s_1 \sin s_1 L) = 0 \tag{47}$$

Eq. 47 is complex, so we follow the same procedure stated before to find the natural frequencies.

3.1.9 F-MS boundary condition

The BCs for this case are:

$$\frac{du(0,t)}{dx} - \ell^2 \frac{\partial^3 u(0,t)}{\partial x^3} = 0 \tag{48a}$$

$$\frac{du(0,t)}{dx} = 0 \tag{48b}$$

$$EA\left(\frac{du(L,t)}{dx} - \ell^2 \frac{\partial^3 u(L,t)}{\partial x^3}\right) = -Ku(L,t) - M\frac{\partial^2 u(L,t)}{\partial t^2} \tag{48c}$$

$$\frac{du(L,t)}{dx} = 0 \tag{48d}$$

Applying the BCs of Eqs. 48a-48b to Eq. 18a leads to: $c_2 = c_4 = 0$.
So, Eq. 18a becomes:

$$U(x) = c_1 \cos s_1 x + c_3 \cosh s_2 x \tag{38}$$

Applying the BCs of Eqs. 48c-48d to Eq. 38 and 15 leads to:

$$\begin{bmatrix} C_{11} & C_{12} \\ C_{21} & C_{22} \end{bmatrix} \begin{bmatrix} c_1 \\ c_3 \end{bmatrix} = \begin{bmatrix} 0 \\ 0 \end{bmatrix} \tag{49}$$

where

$C_{11} = -EAs_1 \sin s_1 L\,(1 + \ell^2 {s_1}^2) + K \cos s_1 L - M\omega^2 \cos s_1 L$

$C_{12} = EAs_2 \sinh s_2 L\,(1 - \ell^2 {s_2}^2) + K \cosh s_2 L - M\omega^2 \cosh s_2 L$

$C_{21} = -s_1 \sin s_1 L$

$C_{22} = s_2 \sinh s_2 L$

For a nontrivial solution, the determinant of the coefficient matrix of Eq. 49 must be equal to zero.
So, it is derived the characteristic equation from which the natural frequencies of the F-MS bar can be obtained:

$$\begin{aligned}\left(-EAs_1 \sin s_1 L\,(1 + \ell^2 {s_1}^2) - \cos s_1 L\,(M\omega^2 - K)\right)(s_2 \sinh s_2 L) \\ + \left(EAs_2 \sinh s_2 L\,(1 - \ell^2 {s_2}^2) - \cosh s_2 L\,(M\omega^2 - K)\right)(s_1 \sin s_1 L) = 0\end{aligned} \tag{50}$$

Eq. 50 is complex, so we follow the same procedure stated before to find the natural frequencies.

3.2 Numerical examples

Numerical examples are presented here to show the effects of various parameters, like the ratio of the internal length ℓ to the length of the bar L, the mode number n, the different BCs, the attached mass M, and the attached spring K, on the natural LFs of the GradEla bars with different BCs. The parameters that are used are $E = 1GPa$, $A = 1\,\mu m^2$, and $\rho = 2000\,kg/m^3$.

Figs. 2-10 shows the influence of the above parameters on the LFs of the GradEla bar for the C-F, C-C, F-F, C-M, C-S, C-MS, F-M, F-S, and F-MS cases, respectively.

From Figs. 2-4, is observed that the LFs of the GradEla bar are greater than those predicted by the classical theory. By the increase of the ratio ℓ/L the frequencies increase. That confirms that the GradEla bar model predicts a stiffer bar than the classical theory's one. It is also noticed that the difference between the two models' results is more noticeable for higher modes.

Studying Figs. 5-7 similar results with the C-F case are observed when the attached mass and spring take zero values. Also, by the increase of the ratio M/m the frequencies decrease, and by the increase of the ratio K/k the frequencies increase. While, the frequencies decrease with the simultaneous increase of the ratios M/m and K/k.

From Fig. 8 similar results with the F-F case are observed when the attached mass takes zero values. Also, by the increase of the ratio M/m the frequencies decrease.

From Fig. 9 it is observed that the frequencies increase by the increase of the ratio K/k.

While, from Fig. 10 it is observed that the first frequency increases and the second one decreases by the simultaneous increase of the ratios M/m and K/k.

Fig. 11 compares all the above BCs on the influence of the ratio ℓ/L, and the mode number n, on the LFs of the GradEla bar.

In a general manner, it can be observed that the LFs increase by increasing the ratio ℓ/L, and the mode number n. In addition, it can be seen that the size effects are most prominent for the F-M BCs. Also, the LFs of the C-C and F-F BCs are equal.

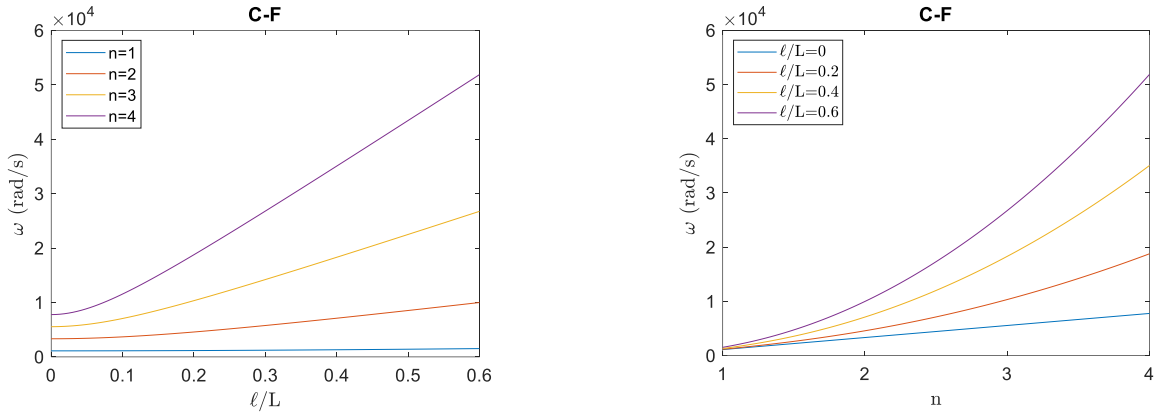

Fig. 2. Influence of the ratio ℓ/L, and the mode number n, on the LFs of the C-F GradEla bar

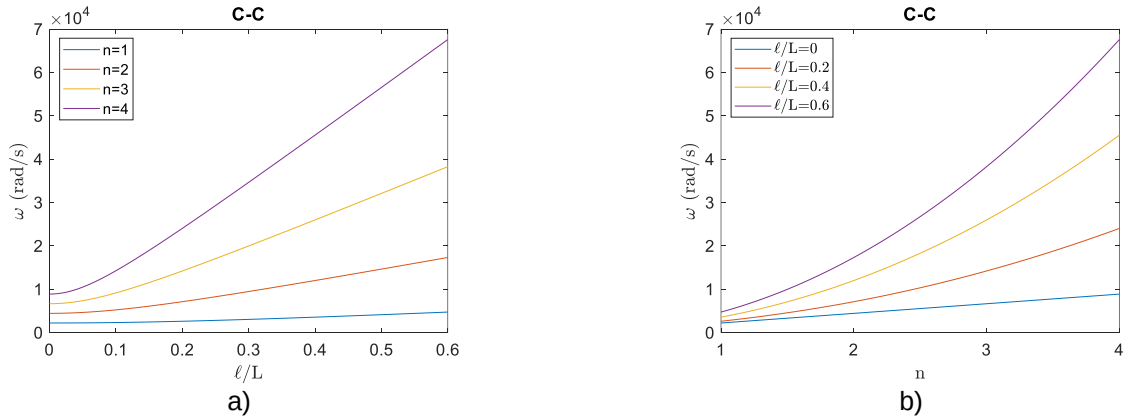

Fig. 3. Influence of the ratio ℓ/L, and the mode number n, on the LFs of the C-C GradEla bar

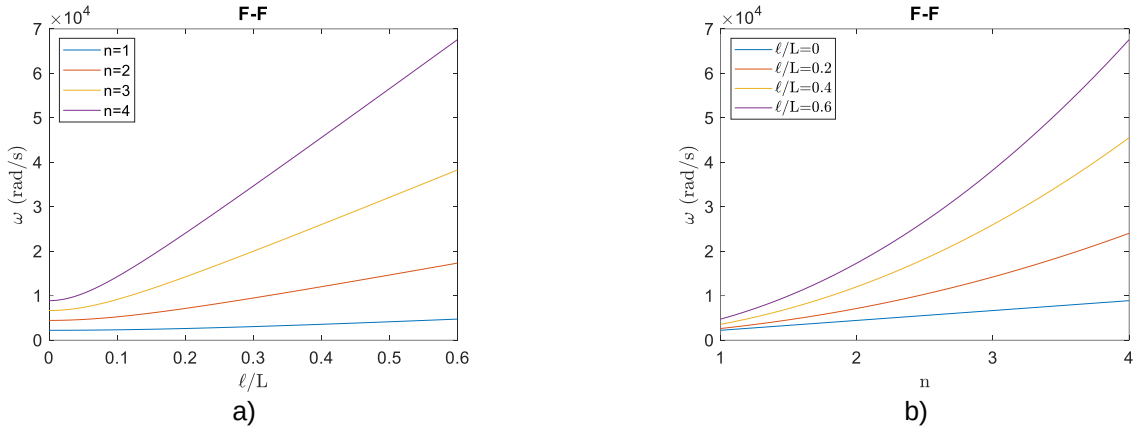

Fig. 4. Influence of the ratio ℓ/L, and the mode number n, on the LFs of the F-F GradEla bar

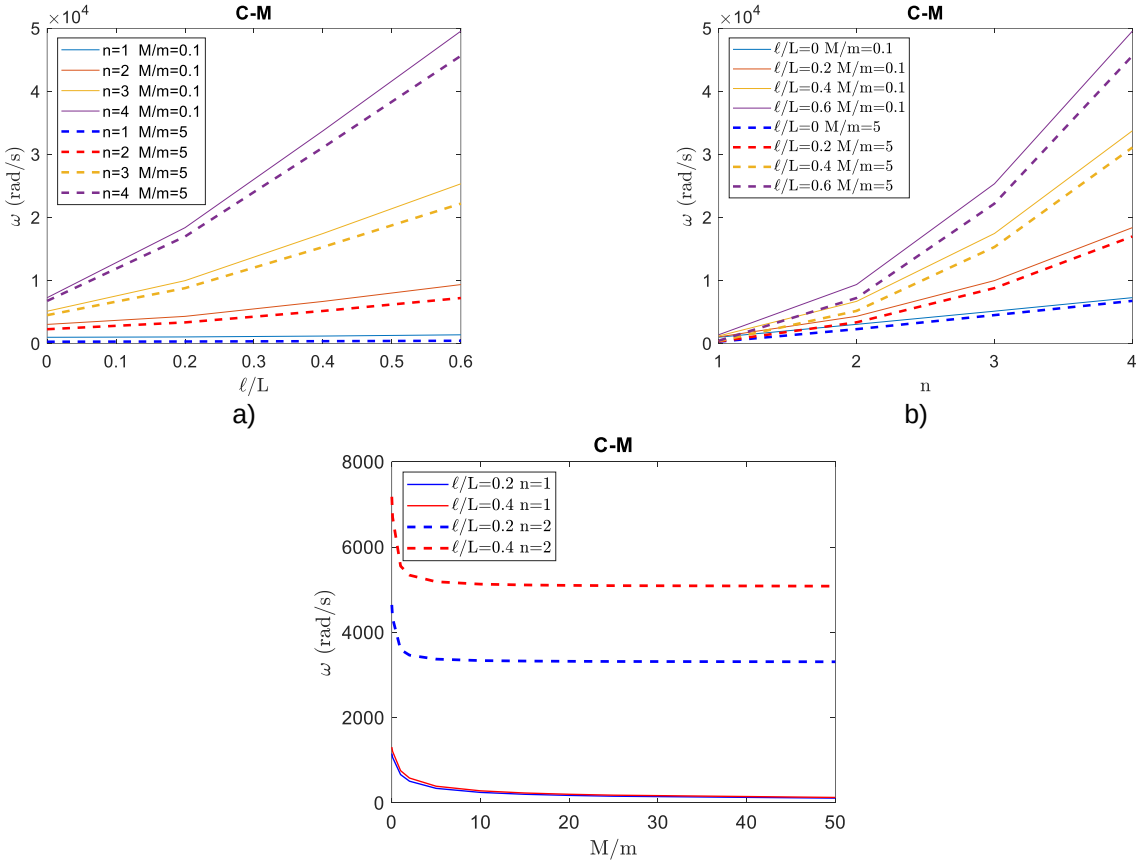

Fig. 5. Influence of the ratio ℓ/L, the mode number n, and the ratio M/m, on the LFs of the C-M GradEla bar

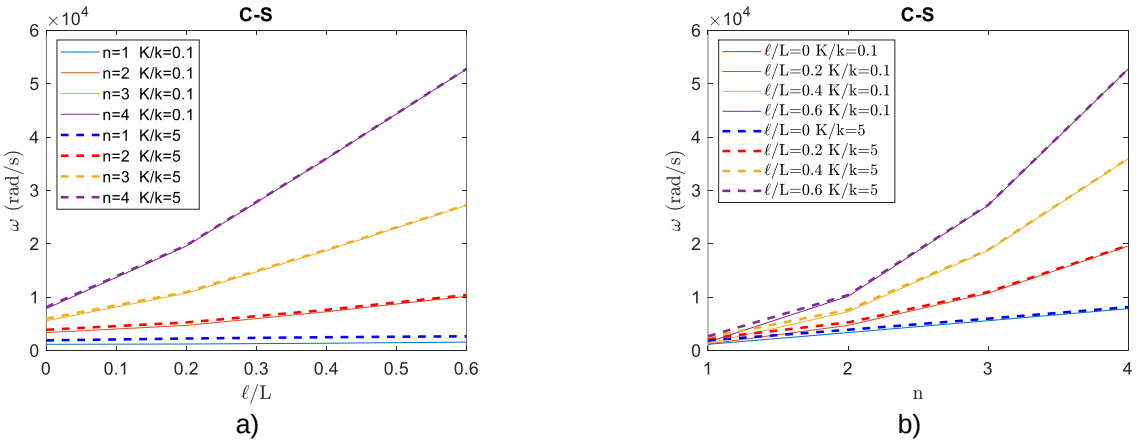

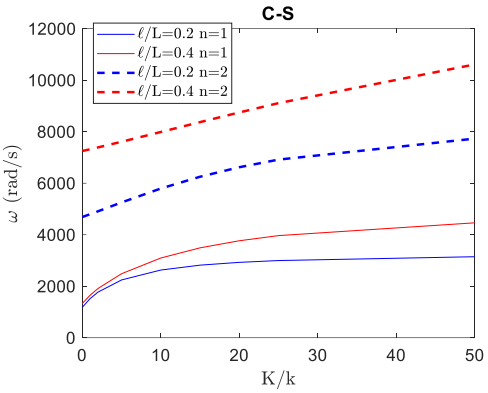

c)

Fig. 6. Influence of the ratio ℓ/L, the mode number n, and the ratio K/k, on the LFs of the C-S GradEla bar

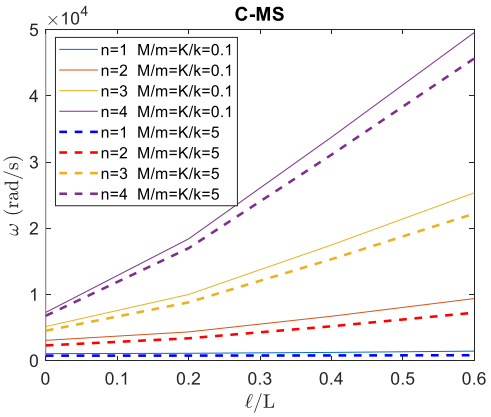

a)

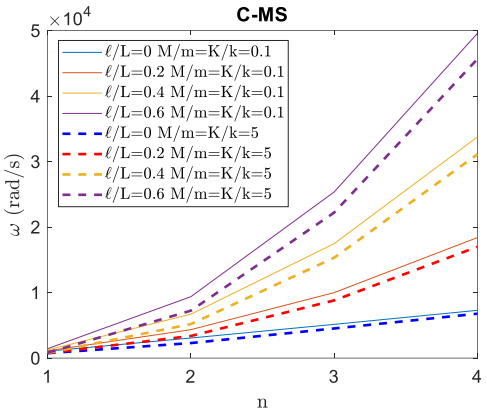

b)

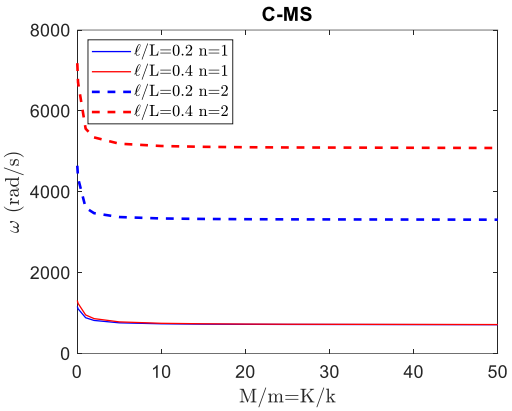

c)

Fig. 7. Influence of the ratio ℓ/L, the mode number n, and the ratios M/m and K/k, on the LFs of the C-MS GradEla bar

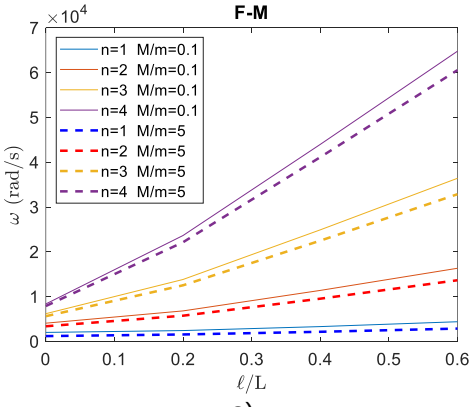

a)

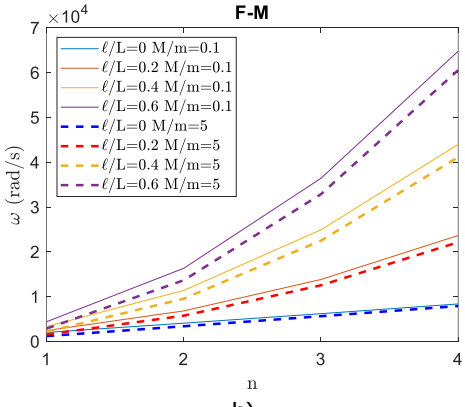

b)

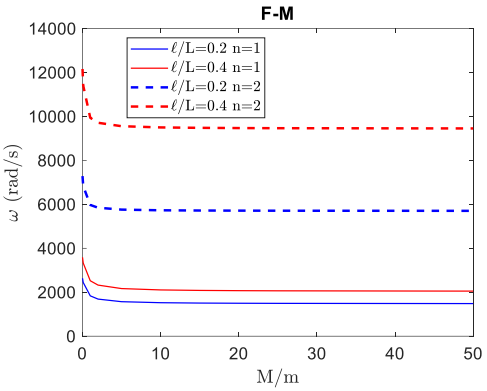

c)

Fig. 8. Influence of the ratio ℓ/L, the mode number n, and the ratio M/m, on the LFs of the F-M GradEla bar.

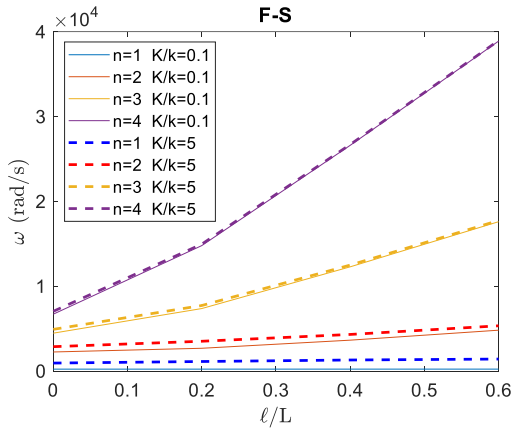

a)

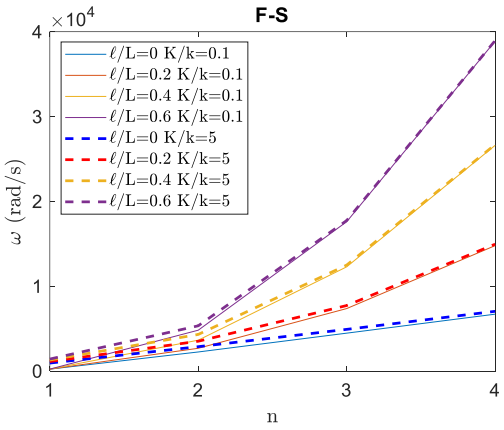

b)

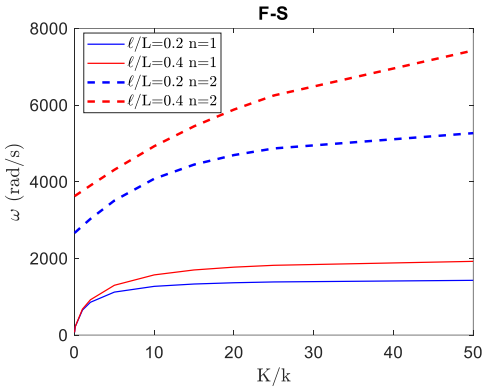

c)

Fig. 9. Influence of the ratio ℓ/L, the mode number n, and the ratio K/k, on the LFs of the F-S GradEla bar

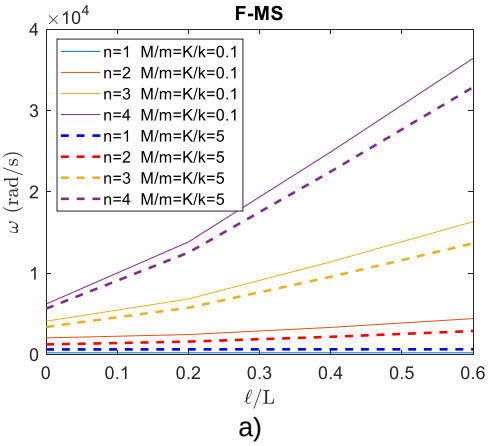

a)

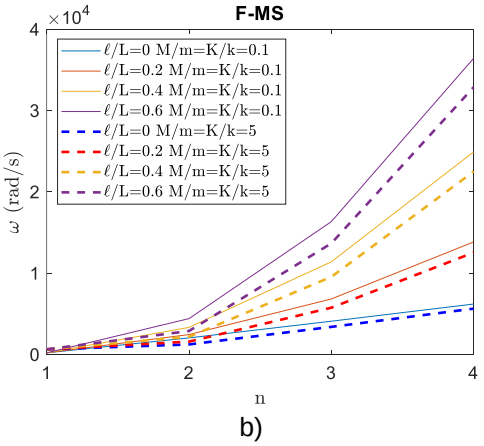

b)

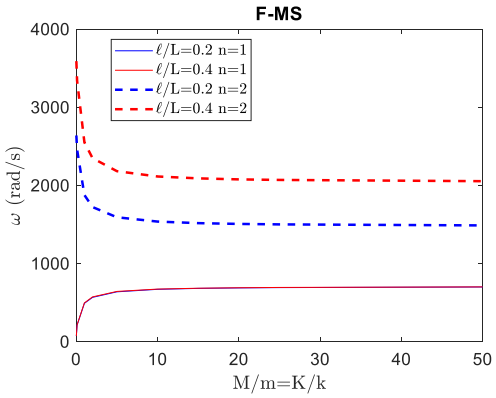

c)

Fig. 10. Influence of the ratio ℓ/L, the mode number n, and the ratios M/m and K/k, on the LFs of the F-MS GradEla bar

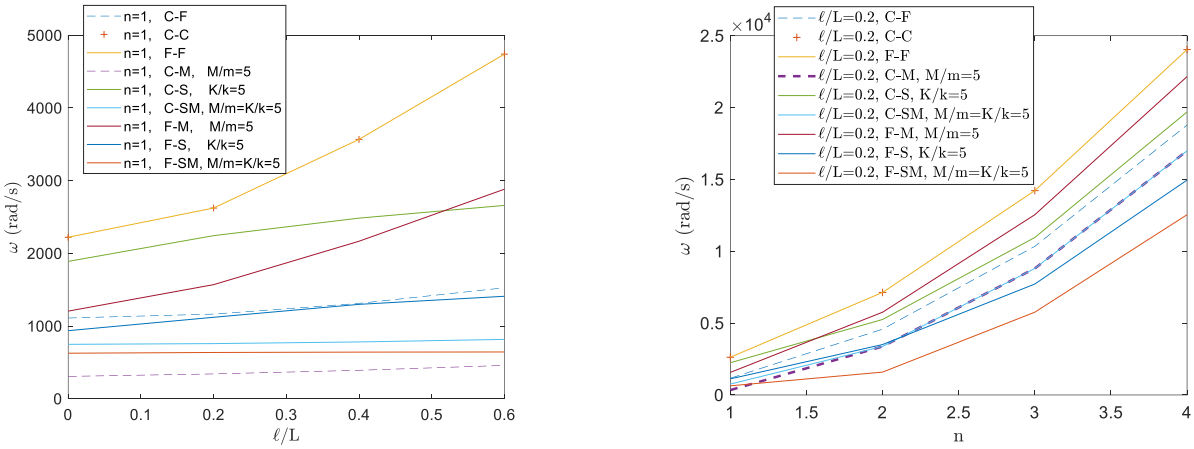

a) b)

Fig. 11. Influence of the different types of BCs on the LFs of the GradEla bar, for different values of the ratio ℓ/L and the mode number n

The presentation of these novel solutions has potential general application to various bar problems. Problems of nanorods, pylons in wind farms, electric wires pylons, telecommunication equipment, or lighting posts, could benefit from these solutions.

3.3 Experimental validation

To get further insight into the use of the GradEla theory and examine its accuracy and validity in real engineering problems, the GradEla theory is applied to predict the LVs of an experiment from the literature [30]. A thin cylindrical steel bar with length $L = 0.7015\,m$, diameter $D = 0.01165\,m$, mass $m = 0.5782\,kg$, and density $\rho = 7732.3\,kg/m^3$, which is free at both ends is subjected to a free vibration. The elastic modulus is assumed to be $E = 200\,GPa$, which is a typical literature value for steel, while the internal length is taken equal to $\ell = 5.82\,mm$, which is a value equal to the radius of the bar.

The LFs versus n are plotted in Fig. 12 for both the classical and the GradEla cases and compared with the experimental ones. Furthermore, the results are depicted in Table 1 along with the error for each case. It is proved that the GradEla case has better accuracy, i.e. $0.36\,\%$ error, compared to the classical one, i.e. $0.64\,\%$ error, especially for modes 3 to 5.

Table 1. LFs for both classical and GradEla cases along with the error

n	Exp. results	Class. Frequency (Error %)	GradEla Frequency (Error %)
1	3649.9	3624.9 (0.68)	3626.2 (0.65)
2	7297.1	7249.9 (0.65)	7259.8 (0.51)
3	10944.3	10874.8 (0.63)	10908.1 (0.33)
4	14591.4	14499.8 (0.63)	14578.6 (0.09)
5	18235.9	18124.8 (0.61)	18278.3 (0.23)
	Avg.Error=	0.64 %	0.36 %

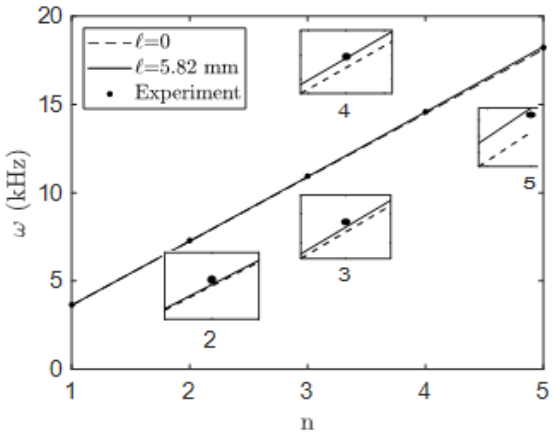

Fig. 12. Longitudinal frequencies versus n for both the classical and the strain gradient cases compared with the experiment [30]

4 CONCLUSIONS

The GradEla theory is employed, in this paper, to study the LFV behavior of bar with several BCs. The governing equation of motion of gradient elastic bars is derived via Hamilton's principle. The equation of motion is solved for various combinations of BCs like clamped, free, attached mass and/or spring. It is noted that many of these solutions are the first in the literature for the GradEla bars. Various applications of bar problems under vibration can benefit from these solutions. It is investigated the effect of the internal length parameter, the modes, the attachments, the BCs, and the length of the bar. It is concluded that the GradEla bar is size-dependent and stiffer, and thus its LFs are greater, compared with the classical one. The difference between the gradient and classical frequencies increases by increasing the mode number and gradient elastic parameter. In addition, the inclusion of the attached mass and spring mainly decreases and increases, respectively, the LFs of bars, while the simultaneous increase of the mass and spring decreases its LFs. Also, it is concluded that the size effects are most noticeable for the F-M BC, while the LFs of the C-C and F-F ones are equal. Finally, the use of GradEla mechanics is shown in a real experiment found in the literature, further emphasising its usefulness in real vibration problems.

5 REFERENCES

[1] Papamichos, E. and Van Den Hoek, P.J. (1995). Size dependency of Castlegate and Berea sandstone hollow-cylinder strength on the basis of bifurcation theory. in 35th U.S. Symposium on Rock Mechanics, USRMS 1995.

[2] Papanastasiou, P.C. and Vardoulakis, I.G. (1989). Bifurcation analysis of deep boreholes: II. Scale effect. Int J Numer Anal Methods Geomech, vol. 13, no. 2, 183-198, doi: 10.1002/nag.1610130206.

[3] Cosserat, E. and Cosserat, F. (1909). Théorie des Corps déformables. Nature, vol. 81, no. 2072, 67-67, doi: 10.1038/081067a0.

[4] Mindlin, R.D. and Tiersten, H.F. (1962). Effects of couple-stresses in linear elasticity. Arch Ration Mech Anal, vol. 11, no. 1, 415-448, doi: 10.1007/BF00253946.

[5] Toupin, R.A. (1962). Elastic materials with couple-stresses. Arch Ration Mech Anal, vol. 11, no. 1, 385-414, doi: 10.1007/BF00253945.

[6] Mindlin, R.D. (1964). Micro-structure in linear elasticity. Arch Ration Mech Anal, vol. 16, no. 1, 51-78, doi: 10.1007/BF00248490.

[7] Mindlin, R.D. (1965). Second gradient of strain and surface-tension in linear elasticity. Int J Solids Struct, vol. 1, no. 4, 417-438, doi: 10.1016/0020-7683(65)90006-5.

[8] Mindlin, R.D. and Eshel, N.N. (1968). On first strain-gradient theories in linear elasticity. Int J Solids Struct, vol. 4, no. 1, 100-124, doi: 10.1016/0020-7683(68)90036-X.

[9] Kröner, E. (1967). Elasticity theory of materials with long range cohesive forces. Int J Solids Struct, vol. 3, no. 5, 731-742, doi: 10.1016/0020-7683(67)90049-2.

[10] Eringen, A.C. and Edelen, D.G.B. (1972). On Nonlocal Elasticity. Int J Eng Sci, vol. 10, no. 3, 233-248, doi: https://doi.org/10.1016/0020-7225(72)90039-0.

[11] Eringen, A.C. (1983). On differential equations of nonlocal elasticity and solutions of screw dislocation and surface waves. J Appl Phys, vol. 54, no. 9, 4703-4710, doi: 10.1063/1.332803.

[12] Yang, F., Chong, A.C.M., Lam, D.C.C., Tong, P. (2002). Couple stress based strain gradient theory for elasticity. Int J Solids Struct, vol. 39, no. 10, 2731-2743, doi: 10.1016/S0020-7683(02)00152-X.

[13] Lam, D.C.C., Yang, F., Chong, A.C.M., Wang, J., Tong, P. (2003). Experiments and theory in strain gradient elasticity. J Mech Phys Solids, vol. 51, no. 8, 1477-1508, doi: 10.1016/S0022-5096(03)00053-X.

[14] Triantafyllidis, N. and Aifantis, E.C. (1986). A gradient approach to localization of deformation. I. Hyperelastic materials. J Elast, vol. 16, no. 3, 225-237, doi: 10.1007/BF00040814.

[15] Aifantis, E.C. (1992). On the role of gradients in the localization of deformation and fracture. Int J Eng Sci, vol. 30, no. 10, 1279-1299, doi: 10.1016/0020-7225(92)90141-3.

[16] Altan, S.B. and Aifantis, E.C. (1992). On the structure of the mode III crack-tip in gradient elasticity. Scripta Metallurgica et Materiala, vol. 26, no. 2, 319-324, doi: 10.1016/0956-716X(92)90194-J.

[17] Altan, B.S., Evensen, H.A., Aifantis, E.C. (1996). Longitudinal vibrations of a beam: A gradient elasticity approach. Mech Res Commun, vol. 23, no. 1, 35-40, doi: 10.1016/0093-6413(95)00074-7.

[18] Tsepoura, K.G., Papargyri-Beskou, S., Polyzos, D., Beskos, D.E. (2002). Static and dynamic analysis of a gradient-elastic bar in tension. Archive of Applied Mechanics, vol. 72, no. 6–7, 483-497, doi: 10.1007/s00419-002-0231-z.

[19] Parisis, K., Dimosthenis, V., Kouris, L., Konstantinidis, A., Aifantis, E.C. (2022). A Note on Gradient/Fractional One-Dimensional Elasticity and Viscoelasticity. Fractal and Fractional, vol. 6, no. 2, 84, doi: 10.3390/fractalfract6020084.

[20] Pisano, A.A. and Fuschi, P. (2003). Closed form solution for a nonlocal elastic bar in tension. Int J Solids Struct, vol. 40, no. 1, 13-23, doi: 10.1016/S0020-7683(02)00547-4.

[21] Aydogdu, M. (2009). Axial vibration of the nanorods with the nonlocal continuum rod model. Physica E Low Dimens Syst Nanostruct, vol. 41, no. 5, 861-864, doi: 10.1016/j.physe.2009.01.007.

[22] Benvenuti, E. and Simone, A. (2013). One-dimensional nonlocal and gradient elasticity: Closed-form solution and size effect. Mech Res Commun, vol. 48, 46-51, doi: 10.1016/j.mechrescom.2012.12.001.

[23] Zhu, X. and Li, L. (2017). On longitudinal dynamics of nanorods. Int J Eng Sci, vol. 120, 129-145, doi: 10.1016/j.ijengsci.2017.08.003.

[24] Numanoğlu, H.M., Akgöz, B., Civalek, O. (2018). On dynamic analysis of nanorods. Int J Eng Sci, vol. 130, 33-50, doi: 10.1016/j.ijengsci.2018.05.001.

[25] Kahrobaiyan, M.H., Asghari, M., Ahmadian, M.T. (2013). Longitudinal behavior of strain gradient bars. Int J Eng Sci, vol. 66–67, 44-59, doi: 10.1016/j.ijengsci.2013.02.005.

[26] Akgöz, B. and Civalek, O. (2014). Longitudinal vibration analysis for microbars based on strain gradient elasticity theory. JVC/Journal of Vibration and Control, vol. 20, no. 4, 606-616, doi: 10.1177/1077546312463752.

[27] Aifantis, E.C. (1984). On the microstructural origin of certain inelastic models. Journal of Engineering Materials and Technology, Transactions of the ASME, vol. 106, no. 4, 326, doi: 10.1115/1.3225725.

[28] Aifantis, E.C. (1987). The physics of plastic deformation. Int J Plast, vol. 3, no. 3, 211-247, doi: 10.1016/0749-6419(87)90021-0.

[29] Ru, C.Q. and Aifantis, E.C. (1993). A simple approach to solve boundary-value problems in gradient elasticity. Acta Mech, vol. 101, no. 1–4, 59-68, doi: 10.1007/BF01175597.

[30] Velasco, S., Román, F.L., White, J.A. (2010). A simple experiment for measuring bar longitudinal and flexural vibration frequencies. Am J Phys, vol. 78, no. 12, 1429-1432, doi: 10.1119/1.3493403.

Paper submitted: 05.06.2024.

Paper accepted: 19.08.2024.